Role of the Invariant Peptide Fragment Forming NH···S Hydrogen Bonds in the Active Site of Cytochrome P-450 and Chloroperoxidase: Synthesis and Properties of Cys-Containing Peptide Fe(III) and Ga(III) (Octaethylporphinato) Complexes as Models

Takafumi Ueno, Nami Nishikawa, Shino Moriyama, Seiji Adachi, Keonil Lee, Taka-aki Okamura, Norikazu Ueyama,* and Akira Nakamura*

Department of Macromolecular Science, Graduate School of Science, Osaka University, Toyonaka, Osaka 560-0043, Japan

Received June 22, 1998

The primary sequence of Cys-X-Gly-Y− (X, hydrophobic residue; Y, hydrophilic residue) is highly conserved in cytochrome P-450s. The amide NHs of Leu, Gly, and X are assumed to form NH···S hydrogen bonds which are also found in the active site fragment, Cys-Pro-Ala-Leu, of chloroperoxidase (CPO). [Fe^{III}(OEP)(Z-**cys**-Leu-Gly-Leu-OMe)] (OEP, octaethylporphinato; Z, benzyloxycarbonyl) and [Fe^{III}(OEP)(Z-**cys**-Pro-Ala-Leu-OMe)] were synthesized as P-450 and CPO model complexes containing the invariant amino acid fragment of the active site. The corresponding gallium(III) complexes were also synthesized to investigate the solution structures using two-dimensional (2D) NMR experiments because the Ga(III) ion is similar to the Fe(III) ion in the ionic radii and in the coordination geometry. The solution structures of the peptide part of the gallium complexes indicate that the invariant fragments maintain a β I-turn−like conformation and then form NH···S hydrogen bonds between S^{γ}Cys and NH of the third and fourth amino acid residues. The hydrogen bonds have also been confirmed by the ^{2}H NMR spectra of N^{2}H-substituted Fe(III) peptide complexes. The Fe^{III}/Fe^{II} redox potentials of the Fe(III) complexes indicate that the NH···S hydrogen bonds in the fragments causes a slight positive shift of the redox potential. The tri- and tetrapeptide Fe(III) complexes containing the invariant fragments of P-450 are kinetically stable at 30 °C in CH_2Cl_2. In contrast, [Fe^{III}(OEP)(Z-**cys**-Leu-OMe)] decomposed to give [Fe^{II}(OEP)] (22%) and the corresponding disulfide immediately in CD_2Cl_2 at 30 °C for 1 h. These results indicate that the invariant fragments involving the hydrogen bonds cause the stabilization of the high-spin Fe(III) resting state rather than the positive shift of Fe^{III}/Fe^{II} redox potential.

Introduction

The heme-thiolate proteins are involved in a wide range of biological oxidations, including epoxidations, hydroxylations, heteroatom oxidation, and halogenations.[1,2] The most distinctive feature in the structure of the proteins is the coordination of a thiolate anion, from proximal cysteine residue, to the heme iron as a fifth ligand. Although cytochrome P-450cam (P-450cam) and chloroperoxidase (CPO) are well-known as the heme-thiolate proteins, the two enzymes have rather distinct catalytic properties; P-450cam is a monooxygenase that activates dioxygen for O-atom insertion into inert C−H bonds, whereas CPO exhibits classic peroxidase and catalase activities and can also catalyze the peroxide-dependent halogenation of organic substrates. Clearly, the catalytic activity of each of these enzymes must be influenced by structure of the protein environment surrounding the Fe−S bonding.[3,4]

The cysteinyl thiolate ligation as the axial ligand is essential for their catalytic cycles, for which the reaction mechanism has already been proposed by the investigations of model complexes and native enzymes.[5] The role of the cysteinate proximal ligand of P-450 has suggested a strong internal electron donor to promote O−O bond cleavage in the putative ferric-peroxide intermediate to generate the proposed ferryl-oxo "active oxygen" state of the reaction cycle.[5−8] In addition, the P-450 model reaction study by Higuchi et al.[9,10] suggested that the thiolate ligand enhances heterolytic cleavage of the peroxy acid iron porphyrin complex even in highly hydrophobic media. Recently, CPO model reactions by arenethiolate model complexes has also been reported.[11] Although the importance of cysteinyl ligand has been indicated by spectroscopic investigations and reactions of the thiolate model complexes,[8−24] it was impossible in these

* Corresponding authors.

(1) In this paper, small bold "**cys**" is used for the residue coordinating to a metal ion.

(2) Ortiz de Montellano, P. R. *Cytochrome P450 Structure, Mechanism, and Biochemistry*; Plenum Press: New York, 1995.
(3) Sundaramoorthy, M.; Terner, J.; Poulos, T. L. *Structure* **1995**, *3*, 1367−1377.
(4) Poulos, T. L.; Finzel, B. C.; Howard, A. J. *J. Mol. Biol.* **1987**, *195*, 687−700.
(5) Dawson, J. H. *Science* **1988**, *240*, 435−439.
(6) Dawson, J. H.; Sono, M. *Chem. Rev.* **1987**, *87*, 1255−1276.
(7) Liu, H. I.; Sono, M.; Kadkhodayan, S.; Hager, L. P.; Hedman, B.; Hodgson, K. O.; Dawson, J. H. *J. Biol. Chem.* **1995**, *2270*, 10544−10550.
(8) Dawson, J. H.; Holm, R. H.; Trudell, J. R.; Barth, G.; Linder, R. E.; Bunnenberg, E.; Djerassi, C.; Tang, S. C. *J. Am. Chem. Soc.* **1976**, *98*, 3707−3709.
(9) Higuchi, T.; Uzu, S.; Hirobe, M. *J. Am. Chem. Soc.* **1990**, *112*, 7051−7053.
(10) Higuchi, T.; Shimada, K.; Maruyama, N.; Hirobe, M. *J. Am. Chem. Soc.* **1993**, *115*, 7551−7552.
(11) Wagenknecht, H.-A.; Woggon, W.-D. *Angew. Chem., Int. Ed. Engl.* **1997**, *36*, 390−392.
(12) Stäubli, B.; Fretz, H.; Piantini, U.; Woggon, W.-D. *Helv. Chim. Acta* **1987**, *70*, 1173−1193.
(13) Ueyama, N.; Nishikawa, N.; Yamada, Y.; Okamura, T.; Nakamura, A. *J. Am. Chem. Soc.* **1996**, *118*, 12826−12827.

10.1021/ic980710u CCC: $18.00
Published on Web 02/26/1999

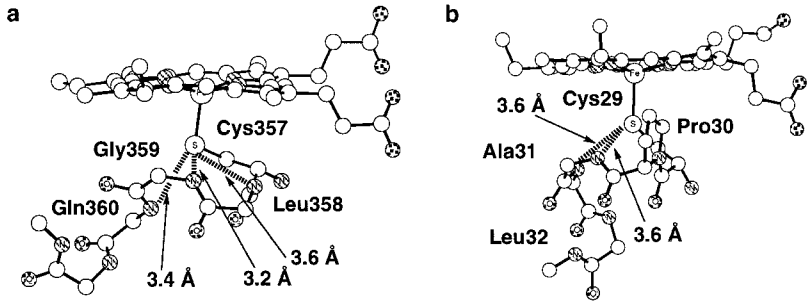

Figure 1. Structures of the cysteinato ligand in (a) P-450cam[25] and (b) CPO.[3] Broad dashed lines indicate the NH···S hydrogen bonds between the cysteinyl sulfur and backbone nitrogen atoms. Boldface numbers show the distances between the cysteine sulfur and the nitrogen of peptide amide groups.

model studies to clarify the variation of the cysteinyl basicity by the peptide conformation.

The crystal structure of P-450cam indicates that a hydrophobic environment called "cys-pocket" has been kept around Cys357. The cysteinyl sulfur atom which is on the N terminus of the L-helix is suggested to form NH···S hydrogen bonds with amide protons of Leu358, Gly359, and Gln360 (Figure 1a).[25] Comparison among the structures of three P-450s shows that the peptide conformation, from the cys-pocket to the L-helix, has the lowest root-mean-square deviation (RMSD) among them.[26] It is suggested that the NH···S hydrogen bond and α-helix are both essential to regulate the Fe−S bond of P-450. CPO also has the NH···S hydrogen bonds and the cysteinyl residue on the N terminus of α-helix based on the X-ray crystal structural analysis (Figure 1b).[3] The number of NH···S hydrogen bonds is different from that of P-450, however. Therefore, the hairpin turn depending on the amino acid sequence must contribute to the activation of small molecules and the redox reaction at the Fe−S bond. P-450cam without the sixth ligand[25] has shorter NH···S hydrogen bond distances than the P-450cam containing C═O[27] or H_2O[28] as sixth ligands found in the crystal structures. These results mean that the binding of substrates or small molecules makes the polypeptide conformational change of the active site. Hence, the primary sequences, Cys-Leu-Gly-X (P-450) and Cys-Pro-Ala-Leu (CPO), are important to understand the catalytic reaction of P-450 and CPO, respectively. In addition, the existence of such NH···S hydrogen bonding at the active sites of various kinds of metalloproteins, e.g., ferredoxin,[29] nitrogenase,[30] has been suggested in their crystallographic reports. Thus, the amino acid sequences containing the NH···S hydrogen bonds contribute to the regulation of the Fe−S bonding of the metalloproteins.

Our attention focused on the invariant sequences that support the formation NH···S hydrogen bonds and we proposed that the unique property of the fragments contributes to the observed catalytic reactivity of P-450 and CPO. Here, we report a new design of cys-containing peptide ligands, Z-Cys-Leu-Gly-Leu-OMe and Z-Cys-Pro-Ala-Leu-OMe, and the synthesis as well as the properties of [Fe^{III}(OEP)(cys-peptide)] (OEP, octaethylporphinato). We had a little information about the hydrogen bond in heme-thiolate proteins based on limited arenethiolate models,[31,32] although several hydrogen-bonded non-heme model complexes have been reported.[33−37] The peptide model complexes of P-450 and CPO are more suitable because the peptide ligands precisely reproduce a part of the active site environment. However, the solution structures of the Fe(III) complexes could not be determined by ^{1}H NMR spectroscopy alone because the complexes are paramagnetic.[38] We used Ga(III) substitution to investigate the solution structure of the peptide complexes. The Ga(III) ion is similar to the Fe(III) ion with the ionic radii and coordination geometry.[39,40] Ga(III) substitution has already been performed for the paramagnetic [Fe_2S_2] ferredoxins to characterize the structural and functional features of the ferric forms of the native iron−sulfur proteins with use of conventional NMR techniques.[41] Thus, gallium compounds have a close structural resemblance to the iron−sulfide−thiolate compound.[40] We have also reported that [Ga^{III}(OEP)(SAr)] is isomorphous with the corresponding [Fe^{III}(OEP)(SAr)].[42] Therefore, we synthesized and characterized [Ga^{III}(OEP)(cys-peptide)] complexes as

(14) Schappacher, M.; Richard, L.; Fischer, J.; Weiss, R.; Bill, E.; Montiel-Montoya, R.; Winkler, H.; Trautwein, A. X. *Eur. J. Biochem.* **1987**, *168*, 419−429.
(15) Schappacher, M.; Richard, L.; Fischer, J.; Weiss, R.; Montiel-Montoya, R.; Bill, E.; Trautwein, A. X. *Inorg. Chem.* **1989**, *28*, 4639−4645.
(16) Byrn, M. P.; Strouse, C. E. *J. Am. Chem. Soc.* **1991**, *113*, 2501−2508.
(17) Collman, J. P.; Sorrell, T. N.; Hoffman, B. M. *J. Am. Chem. Soc.* **1975**, *97*, 913−914.
(18) Koch, S.; Tang, S. C.; Holm, R. H. *J. Am. Chem. Soc.* **1975**, *97*, 916−917.
(19) Koch, S.; Tang, S. C.; Holm, R. H. *J. Am. Chem. Soc.* **1975**, *97*, 914−916.
(20) Miller, K. M.; Strouse, C. E. *Acta Crystallogr., Sect. C* **1984**, *40*, 1324−1327.
(21) Oshio, H.; Ama, T.; Watanabe, T.; Nakamoto, K. *Inorg. Chim. Acta* **1985**, *96*, 61−66.
(22) Miller, K. M.; Strouse, C. E. *Inorg. Chem.* **1984**, *23*, 2395−2400.
(23) Tang, S. C.; Koch, S.; Papaefthymiou, G. C.; Foner, S.; Frankel, R. B.; Ibers, J. A.; Holm, R. H. *J. Am. Chem. Soc.* **1976**, *98*, 2414−2434.
(24) Ogoshi, H.; Sugimoto, H.; Yoshida, Z. *Tetrahedron Lett.* **1975**, *27*, 2289−2292.
(25) Raag, R.; Poulos, T. L. *Biochemistry* **1989**, *28*, 917−922.
(26) Hasemann, C. A.; Kurumbail, R. G.; Boddupalli, S. S.; Peterson, J. A.; Deisenhofer, J. *Structure* **1995**, *2*, 41−62.
(27) Raag, R.; Poulos, T. L. *Biochemistry* **1989**, *28*, 7586−7592.
(28) Poulos, T. L.; Finzel, B. C.; Howard, A. J. *Biochemistry* **1986**, *25*, 5314−5322.
(29) Fukuyama, K.; Matsubara, H.; Tukihara, T.; Katsube, Y. *J. Mol. Biol.* **1989**, *210*, 383−398.
(30) Kim, J.; Woo, D.; Rees, D. C. *Biochemistry* **1993**, *32*, 7104−7115.
(31) Ueyama, N.; Nishikawa, N.; Okamura, T.; Yamada, Y.; Nakamura, A. *Inorg. Chem.* **1998**, *37*, 2415.
(32) Ueyama, N.; Yamada, Y.; Okamura, T.; Kimura, S.; Nakamura, A. *Inorg. Chem.* **1996**, *35*, 6473−6484.
(33) Ueyama, N.; Terakawa, T.; Nakata, M.; Nakamura, A. *J. Am. Chem. Soc.* **1983**, *105*, 7098−7101.
(34) Ueyama, N.; Nakata, M.; Nakamura, A. *Bull. Chem. Soc. Jpn.* **1985**, *58*, 464.
(35) Sun, W.-Y.; Ueyama, N.; Nakamura, A. *Inorg. Chem.* **1991**, *30*, 4026−4030.
(36) Huang, J.; Ostrander, R. L.; Rheingold, A. L.; Leung, Y.; Walters, M. A. *J. Am. Chem. Soc.* **1994**, *116*, 6769−6776.
(37) Huang, J.; Ostrander, R. L.; Rheingold, A. L.; Walters, M. A. *Inorg. Chem.* **1995**, *34*, 1090−1093.
(38) Lukat, G. S.; Goff, H. M. *Biochim. Biophys. Acta* **1990**, *1037*, 351−359.
(39) Shannon, R. D. *Acta Crystallogr., Sect. A* **1976**, *32*, 751−767.
(40) Maelia, L. E.; Koch, S. A. *Inorg. Chem.* **1986**, *25*, 1896−1904.
(41) Vo, E.; Wang, H. C.; Germanas, J. P. *J. Am. Chem. Soc.* **1997**, *119*, 1934−1940.

Table 1. Multiple Sequence Alignment of Various P-450s[a] and CPO[b] Based Primarily on Sequence Conservation

	sequence
P450cam	H**G**SHL**C**L**G**QH
P450terp	W**G**AHM**C**L**G**QH
P450BM3	N**G**QRA**C**I**G**QQ
P450eryF	Q**G**IHF**C**M**G**RP
P450scc	W**G**VRQ**C**V**G**RR
P45026-ohp	Y**G**VRA**C**L**G**RR
P450c21B	C**G**APV**C**L**G**EP
P45017a	A**G**PRS**C**I**G**EA
P450d	L**G**KRR**C**I**G**EI
P450M1	A**G**KRI**C**A**G**EA
P450PBc4	A**G**KRM**C**V**G**EG
P4503a	A**G**KRV**C**V**G**EG
P450b	T**G**KRI**C**L**G**EG
P45015aoh-1	I**G**KRY**C**F**G**EG
P450nf-25	S**G**PRN**C**I**G**MR
P450Arom	F**G**PRG**C**A**G**KY
CPO	DSRAP**C**PALN

Fe(III) five-coordinate P-450 and CPO structural models to elucidate the role of invariant fragments of the heme-thiolate proteins by systematic investigation of Fe(III) and Ga(III) cys-containing peptide model complexes.

Results

Design of Peptide Ligand. The primary sequences around the cysteine residue ligating to the iron atom of various P-450s[26,43] and CPO[44] were shown in Table 1. The fragments after the cysteine residue were highly conserved in P-450s. The residue next to the cysteine residue is a hydrophobic amino acid residue, e.g., Leu, Ile, Val, Ala, Met, and Phe. A glycine residue has been kept as the third residue in all the known P-450s. Most of the fourth residues can be classified as a hydrophilic residue, e.g., Gln, Glu, and Arg. On the other hand, some residues just before the Cys indicate little similarity for the P-450s. The structural comparison among P-450cam, P-450terp, and P-450BM-3 indicates that the structure around the invariant cysteine residue has the lowest RMSD among the three structures.[26] Thus, the cysteine residue exists in the hydrophobic environment. Recently, the formation of the NH···S hydrogen bond between the cysteinyl sulfur atom and NHs of the leucine and glycine residues was suggested.[45] We estimated that the sequence of Cys-X-Gly-Y (X, hydrophobic amino acid residue; Y, hydrophilic amino acid residue) is important to regulate the activity of P-450s. Therefore, we designed three suitable model peptides: Z-Cys-Leu-Gly-Leu-OMe, Z-Cys-Leu-Gly-OMe, and Z-Cys-Leu-OMe. The first leucine residue was chosen as the highest conserved residue at the position in Table 1. The second leucine residue was used because of the peptide solubility for synthesis and ease in characterization of the model complexes in CH_2Cl_2, although this position has been occupied by a hydrophilic residue in most of the native P-450s.

The sequence around the cysteine residue bonding to the heme is -Pro-Cys-Pro-Ala-Leu- (Table 1) from the crystal structure of CPO.[3] The similarities to the active site of P-450 are the hydrophobic environment and the NH···S hydrogen bonding interactions. In addition, the Cys-Pro-X-Y- fragment has been highly conserved in iron−sulfur proteins, e.g., [4Fe−4S] ferredoxin and rubredoxins.[29,46,47] The crystal structures of the iron−sulfur proteins suggested that the S^{γ} atom of the cysteine residue ligating to the iron makes the NH···S hydrogen bonds with NHs of X and Y residues. Therefore, we proposed that the Cys-Pro-Ala-Leu fragment has an important role for the activity of CPO. Thus, we synthesized CPO model peptide ligands, Z-Cys-Pro-Ala-Leu-OMe, Z-Cys-Pro-Leu-OMe, and Z-Cys-Pro-OMe.

We clarified the contribution of the invariant fragments to the peptide conformation and NH···S hydrogen bond in the active sites of P-450s and CPO by the systematic investigation on [M^{III}(OEP)(cys-peptide)] (M = Fe and Ga) having one of the designed cys-containing peptide ligands.

Synthesis. Fe^{III}(OEP)(cys-peptide) Complexes. The synthesis of five-coordinate Fe(III) porphyrin thiolate complexes was reported by several researchers.[23,24,48] In particular, arenethiolate complexes were synthesized by reaction between [Fe^{III}(OEP)]$_2$O and the corresponding thiol.[23] Stable compounds were obtained only with arenethiolates; reaction of the OEP dimer with alkanethiols afforded no isolable Fe(III) products. Alkanethiolate complexes, [Fe^{III}(OEP)(SR)], were synthesized using the methods reported by Ogoshi et al.[24] As a more convenient and versatile method for the synthesis of the cysteine-containing peptide Fe^{III}(OEP) complexes, we used a ligand exchange reaction between [Fe^{III}(OEP)(OMe)] and the corresponding peptide ligand. This method already has been applied for the synthesis of [Fe^{III}(OEP)(SEt)] and [Fe^{III}(OEP)(OPh)].[48] The ligand exchange reaction was completed by evaporation of MeOH under reduced pressure (eq 1).

$$[Fe^{III}(OEP)(OMe)] + \text{Cys-peptide} \rightarrow [Fe^{III}(OEP)(\textbf{cys}\text{-peptide})] + MeOH \quad (1)$$

Starting material, [Fe^{III}(OEP)(OMe)], has been reported by Hatano and Uno.[49] The reaction products, [Fe^{III}(OEP)(cys-peptide)], were characterized by a combination of spectroscopic methods. The observed α−H (32 ppm), *β*−H (5.0 ppm), and *meso* protons (−33 ppm) of [Fe^{III}(OEP)(OMe)] changed to α−H (38−43 ppm), *β*−H (ca. 6 ppm), and *meso* protons (−43 to −46 ppm) in the products, respectively, in CD_2Cl_2 at 30 °C. The ^{1}H NMR data show that the ligand exchange reaction proceeded completely. Electrospray ionization mass spectroscopy (ESI-MS) data for complex **1**−**4** indicate the five-coordinate [Fe^{III}(OEP)(cys-peptide)] structure. Comparisons of the calculated and the observed electrospray mass spectra in the M^+ parent ion region are presented in Figure 2. The agreement of

(42) Okamura, T.; Nishikawa, N.; Ueyama, N.; Nakamura, A. *Chem. Lett.* **1998**, 199.
(43) Cupp-Vickery, J. R.; Poulos, T. L. *Nat. Struct. Biol.* **1995**, *2*, 144−153.
(44) Keningsberg, P.; Fang, G.-H.; Hager, L. P. *Arch. Biochem. Biophys.* **1987**, *254*, 409−415.
(45) Poulos, T. L. *J. Biol. Inorg. Chem.* **1996**, *1*, 356−359.
(46) Fukuyama, K.; Nagahara, Y.; Tukihara, T.; Katsube, Y.; Hase, T.; Matsubara, H. *J. Mol. Biol.* **1988**, *199*, 183−193.
(47) Day, M. W.; Hsu, B. T.; Joshua-Tor, L.; Park, J.-B.; Zhou, Z. H.; Adams, M. W. W.; Rees, D. C. *Protein Sci.* **1992**, *1*, 1494−1507.
(48) Uno, T.; Hatano, K.; Nishimura, Y.; Arata, Y. *Inorg. Chem.* **1990**, *29*, 2803−2807.
(49) Hatano, K.; Uno, T. *Bull. Chem. Soc. Jpn.* **1990**, *63*, 1825−1827.

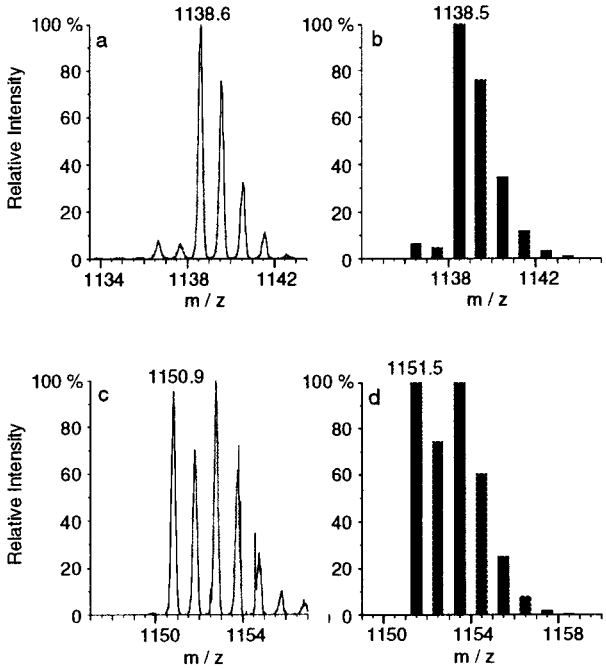

Figure 2. ESI-MS spectra of (a) observed, (b) calculated patterns for {[Fe^{III}(OEP)(Z-**cys**-Pro-Ala-Leu-OMe)] (**3**) + H^+}, (c) observed, and (d) calculated patterns for {[Ga^{III}(OEP)(Z-**cys**-Pro-Ala-Leu-OMe)] (**7**) + H^+} in CH_3CN:CH_2Cl_2 (1:1) (0.2 mM).

the spectra across the entire isotope distribution pattern is excellent and unambiguously establishes the stoichiometries.

Special kinds of the peptide sequences contribute stability of the peptide complexes. The tetra- and the tripeptide complexes containing the invariant fragments of P-450 are kinetically stable at 30 °C in CH_2Cl_2. In a dipeptide complex, [Fe^{III}(OEP)-(Z-cys-Leu-OMe)], it changed to [Fe^{II}(OEP)] (22%) and the cysteine-containing peptide (see eq 2) in CD_2Cl_2 at 30 °C after 1 h because the Z-Cys-Leu-OMe fragment accelerates the reported self-redox reaction (eq 2).[23]

$$[Fe^{III}(OEP)(\text{cys-peptide})] \rightarrow 2[Fe^{II}(OEP)] + \text{peptide-cys-S}-\text{S-cys-peptide} \quad (2)$$

The pK_a values of Z-Cys-Leu-Gly-Leu-OMe, Z-Cys-Leu-Gly-OMe, and Z-Cys-Leu-OMe were 9.9, 9.0, and 11.2, respectively, in micellar solution.[50] Therefore, formation of the corresponding disulfide is easier in Z-Cys-Leu-OMe than Z-Cys-Leu-Gly-Leu-OMe and Z-Cys-Leu-Gly-OMe. The same trend was observed with the CPO model complexes. The peptide sequences, Z-Cys-Leu-Gly-Leu-OMe and Z-Cys-Pro-Ala-Leu-OMe, are thus found to contribute to the kinetic stability of [Fe^{III}(OEP)(cys-peptide)] in CH_2Cl_2.

[Ga^{III}(OEP)(cys-peptide)] Complexes. Synthesis of [Ga^{III}-(OEP)(cys-peptide)] is the first example of the synthesis of alkanethiolate OEP Ga(III) complexes, i.e., [Ga^{III}(OEP)(SR)]. As a more convenient and versatile method for the synthesis of the cys-containing peptide Ga(III) complexes, we used a ligand exchange reaction between [Ga^{III}(OEP)(OMe)] and the corresponding peptide ligand. This method has already been applied for the synthesis of [Ga^{III}(OEP)(SAr)].[42] The ligand exchange reaction was completed by evaporation of MeOH under reduced pressure just in [Fe^{III}(OEP)(cys-peptide)], and the process can be monitored by disappearance of MeO ^{1}H NMR signals at −1.92 ppm in $CDCl_3$ at 30 °C. The five-coordinate Ga(III) peptide complexes were confirmed by the integral ratio between the porphyrin and the peptide ^{1}H NMR signals (data not shown) and ESI-MS (Figure 2).

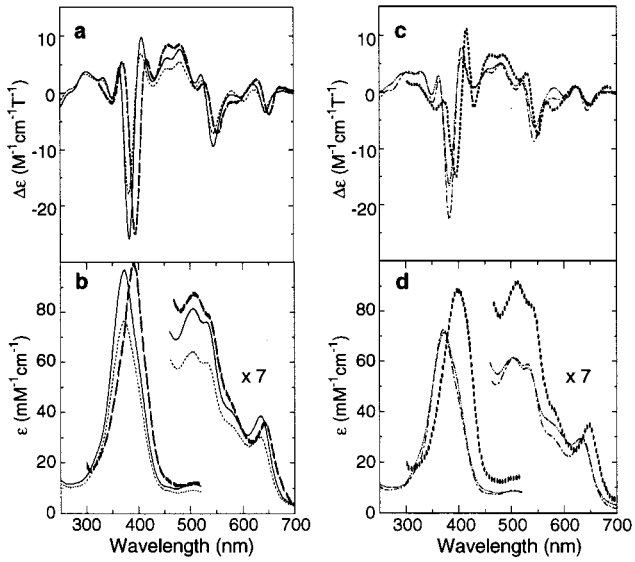

Figure 3. (a) MCD and (b) UV−vis spectra of [Fe^{III}(OEP)(Z-**cys**-Leu-Gly-Leu-OMe)] (**1**) (—), [Fe^{III}(OEP)(Z-**cys**-Leu-Gly-OMe)] (**2**) (- - -) in dichloromethane and P-450cam (high-spin five-coordinated ferric iron) (— —).[8,52] MCD (c) and UV−vis (d) spectra of [Fe^{III}(OEP)-(Z-**cys**-Pro-Ala-Leu-OMe)] (**3**) (— —), [Fe^{III}(OEP)(Z-**cys**-Pro-Leu-OMe)] (**4**) (—···—) and CPO (high-spin five-coordinated ferric iron)[51,52] (···). The spectra were measured in CH_2Cl_2 (0.2 mM) at room temperature.

Electronic and Magnetic Circular Dichroism Spectra. The electronic spectra of the complexes in dichloromethane are shown in Figure 3. Each spectrum consists of an α band near 635 nm, a broad absorption in the β band region containing a shoulder superimposed on a maximum at 505−533 nm, and a Soret band at ca. 370 nm. Thus, all the spectra are clearly the high-spin type.[23,24,48]

The magnetic circular dichroism (MCD) spectra of the model complexes are shown in Figure 3. MCD spectroscopy has already been used to probe the structure of the high-spin ferric states of these two enzymes.[8,51,52] The most important feature of these spectra is the strong negative absorption in the Soret region (ca. 400 nm) common to the peptide model complexes and the native enzymes. The spectral comparison between cys-containing peptide model complexes and the enzymes shows that they are very similar in the visible region, although the comparison between arenethiolate complexes, Fe^{III}(PPIXDME)-(SC_6H_4-*p*-NO_2), and P-450cam is less exact.[8] The results indicate that the peptide model complexes are naturally better than the known arenethiolate model complexes. The absorption and MCD spectra ensure us that complexes **1**−**4** have a high-spin five-coordinate ferric state and the structure around the cysteine residues is similar to that in the active center of P-450 and CPO.

CD Spectra. The identity of peptide conformation for the Fe(III) and Ga(III) peptide complexes was assessed using far UV−CD spectroscopy.[53] The far UV−CD spectra of complexes

(50) Ueno, T.; Moriyama, S.; Ueyama, N.; Nakamura, A. unpublished results.
(51) Dawson, J. H.; Trudell, J. R.; Barth, G.; Linder, R. E.; Bunnenberg, E.; Djerassi, C.; Chiang, R.; Hanger, L. P. *J. Am. Chem. Soc.* **1976**, *98*, 3709−3710.
(52) Sono, M.; Stuehr, D. J.; Ikeda-Saito, M.; Dawson, J. H. *J. Biol. Chem.* **1995**, *270*, 19943−19948.
(53) Rose, G. D.; Gierasch, L. M.; Smith, J. A. *Adv. Protein Chem.* **1985**, *37*, 1−109.

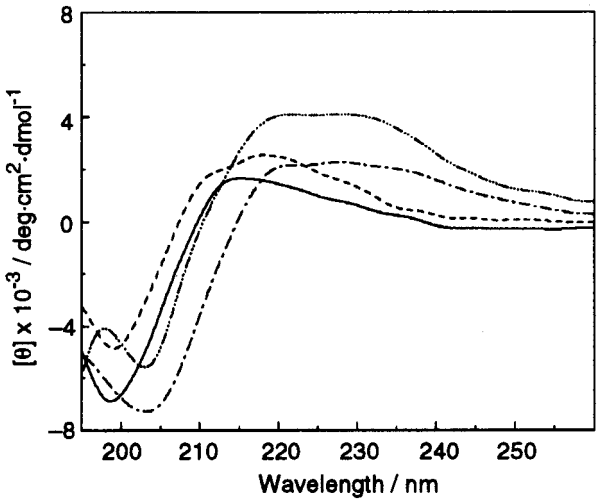

Figure 4. CD spectra of (a) [FeIII(OEP)(Z-**cys**-Leu-Gly-Leu-OMe)] (**1**) (—), [Ga^{III}(OEP)(Z-**cys**-Leu-Gly-Leu-OMe)] (**5**) (- - -), [Fe^{III}(OEP)-(Z-**cys**-Pro-Ala-Leu-OMe)] (**3**) (—•—), and [Ga^{III}(OEP)(Z-**cys**-Pro-Ala-Leu-OMe)] (**7**) (—···) in CH_3CN at 27 °C (2.0 mM).

1, **3**, **5**, **7**, and the corresponding peptides in acetonitrile are shown in Figure 4. **1** and **5** indicate the negative CD band at 199 nm and the positive band near 215 nm. The CD spectra of **3** and **7** exhibit the negative CD band at 203 nm and the positive broad two peaks at 220−240 nm. The spectral pattern of the Ga(III) complexes is similar to the Fe(III) analogues having the same peptide. These results suggest that the peptide conformation of the Fe(III) complexes is similar to that of the corresponding Ga(III) complexes. Therefore, the Ga(III) complexes are suitable as a structural probe to elucidate the unique conformations of the Fe(III) peptide complexes such as Ga(III)-substituted [Fe_2S_2] ferredoxin.[41]

NMR Spectra. Chemical Shifts. A summary of the ^{1}H chemical shifts for the Fe(III) and Ga(III) peptide complexes is given in Table 2. All of the present Fe(III) peptide model complexes have ^{1}H NMR chemical shifts similar to those of reported five-coordinate, high-spin thiolate complexes.[31,54] The broad *meso*, α−H, and β−H resonances occur at ca. −45, +40, and +6 ppm, respectively. The CysC$^\beta$ proton resonances, as well as oxidized P-450 and oxidized CPO,[38] have not been observed from 300 to −100 ppm. Presumably, the resonance is not observed because of the enhanced NMR line broadening and hyperfine-shift of the peaks caused by paramagnetic Fe(III).[55,56]

For the diamagnetic Ga(III) complexes, the chemical shifts of the peptide ligands provide the structural information. Of primary interest are the large upfield shifts experienced by the protons of peptide ligands coordinated to the Ga(III) ion.[55] The space directly above the center of the porphyrin ring should provide the greatest shielding by ring current effect.[57] For example, the resonances of protons of the CysC$^\beta$ in the Ga(III) peptide complexes are observed at −0.5 to −3.5 ppm as reported for [Ru(NO)(OEP)(*S*−NACysMe)].[58] In addition, peaks caused by each of the C$^\alpha$ protons of the third glycine residue appear at 3.42 and 2.15 ppm for [Ga^{III}(OEP)(Z-**cys**-Leu-Gly-Leu-OMe)] (**5**). Two protons of Gly C$^\alpha$ of [Ga^{III}(OEP)(Z-**cys**-Leu-Gly-OMe)] (**6**) are observed as a broad peak at 2.87 ppm at 27 °C. Each of the two Pro C$^\delta$ protons of **7** shows large separations (at 2.42 and 0.17 ppm) (Table 2). The proline side chain prefers a position near the porphyrin ring because of their specific peptide conformation of **7**. Complex **8** also indicates the same trend. These results suggest that the Gly and Pro residues provide considerable interaction between the peptide chain and the porphyrin ring.

An alternative probe for the conformation of the proline residues is given by the ^{13}C chemical shift values of the proline β and γ carbons, because there is little ring current contribution to the ^{13}C chemical shifts of the diamagnetic Ga(III) peptide complexes.[57] Indeed, the C$^\beta$ and C$^\gamma$ chemical shifts of a *trans*-proline are reported at about 29 and 24 ppm in $CDCl_3$, respectively.[59] Complex **8** has the C$^\beta$ and C$^\gamma$ chemical shifts of the proline residue at 28.0 and 23.8 ppm, respectively. Thus, the peptide fragments Cys-Pro in **7** and **8** have *trans*-conformation in $CDCl_3$.

Temperature Dependences of NH Chemical Shifts. The temperature coefficients for amide protons were calculated by a least-squares analysis of the observed temperature dependence of their resonances (Table 3). For [Ga^{III}(OEP)(Z-**cys**-Leu-Gly-Leu-OMe)] (**5**), the temperature coefficients are exceptionally low (0.1−1.3 ppb/K) implying either that they are strongly shielded from the solvent or that they participate in relatively stable hydrogen bonds.[60] On the other hand, the temperature coefficients of Z-Cys-Leu-Gly-Leu-OMe are the highest (10.6−18.3 ppb/K) indicating their probable involvement in intermolecular hydrogen bonding.[61] A similar trend was observed in [Ga^{III}(OEP)(Z-**cys**-Leu-Gly-OMe)] (**6**), [Ga^{III}(OEP)(Z-**cys**-Pro-Ala-Leu-OMe)] (**7**), [Ga^{III}(OEP)(Z-**cys**-Pro-Leu-OMe)] (**8**), and the corresponding peptides. These results show that the conformation of peptide ligands in the Ga(III) complexes has been maintained by intramolecular hydrogen bonds, although the corresponding peptides prefer to form the intermolecular hydrogen bonds because of the absence of the M^{III}(OEP) moiety.

Solution Structures of [Ga^{III}(OEP)(cys-peptide)]. The conformational features of the Ga(III) complexes were assessed by ^{1}H NMR spectroscopy and NMR-restricted molecular mechanics. Although the NMR spectra of paramagnetic Fe(III) complexes feature large line width and poor spectral resolution, the diamagnetic gallium complexes displayed spectra in narrower line widths.[55] Therefore, the 2D experiments for the gallium complexes were carried out[41] because the Ga(III) complexes are without protons having a very short T_1 value (Figure 5).[62] We have also reported that [Ga^{III}(OEP)(SAr)] is isomorphous with the corresponding [Fe^{III}(OEP)(SAr)].[42] Thus, the Ga(III) complexes can provide the solution structures corresponding to the Fe(III) model complexes by the standard 2D NMR methods.[55,63] Our treatment of the Ga(III) ion is described in the Supporting Information. The OEP ligand has been adopted because of its less steric hindrance of the ethyl groups and good separation of the proton peaks of the peptide from the peaks of the porphyrin protons (Table 2).[64] In our calculation, the

(54) Arasasingham, R. D.; Balch, A. L.; Cornman, C. R.; Ropp, J. S. d.; Eguchi, K.; LaMar, G. N. *Inorg. Chem.* **1990**, *29*, 1847−1850.
(55) See Supporting Information.
(56) Xia, B.; Westler, W. M.; Cheng, H.; Meyer, j.; Moulis, J.-M.; Markley, J. L. *J. Am. Chem. Soc.* **1995**, *117*, 5347−5350.
(57) Janson, T. R.; Katz, J. J. *The Porphyrins*; Dolphin, D., Ed.; Academic Press: New York, 1979; Vol. IV, pp 1−59.
(58) Yi, G.-B.; Khan, M. A.; Richter-Addo, G. B. *J. Chem. Soc., Chem. Commun.* **1996**, 2045−2046.
(59) Deber, C. M.; Madison, V.; Blout, E. R. *Acc. Chem. Res.* **1976**, *9*, 106−113.
(60) Stevens, E. S.; Sugawara, N.; Bonora, G. M.; Toniolo, C. *J. Am. Chem. Soc.* **1980**, *102*, 7048−7050.
(61) Pease, L. G.; Watson, C. *J. Am. Chem. Soc.* **1978**, *100*, 1279−1286.
(62) The T_1 values of all protons in the Ga(III) complexes were shown to be 0.2 Å0.6 s by preliminary T_1 measurements.
(63) Wüthrich, K. *NMR of Proteins and Nucleic Acids*; Wiley: New York, 1986.

Table 2. ^{1}H NMR Chemical Shifts (ppm) for [Ga^{III}(OEP)(cys-peptide)] in $CDCl_3$ at 27 °C

complexes	NH[a]	$J_{\alpha N}$ (Hz)	C$^{\alpha}$H	C$^{\beta}$H	C$^{\gamma}$H	C$^{\delta}$H	meso[b]	α-H[b]	β-H[b]
[Ga^{III}(OEP)(Z-**cys**-Leu-Gly-Leu-OMe)] (**5**)[c]							10.33	4.25, 4.10	1.93
							(−43.3)	(38.8)	(6.0)
Cys1	3.31	8.8	0.36	−1.50,					
	(−5.7)			−2.56					
Leu2	3.55	4.4	3.48	1.57,	1.25	0.89,			
	(−18.7)			1.12		0.62			
Gly3	5.62	8.8	3.42,						
	(−9.8)		2.15						
Leu4	5.76	8.9	4.05	1.10,	0.90	0.50,			
	(0.7)		0.92		0.41				
[Ga^{III}(OEP)(Z-**cys**-Leu-Gly-OMe)] (**6**)[d]							10.32	4.24, 4.10	1.93
							(−45.5)	(39.4)	(6.2)
Cys1	3.37	5.6	0.59	−1.76,					
	(−7.2)			−2.44					
Leu2	3.67	−	3.67	1.48,	1.08	0.73,			
	(−18.8)			0.99		0.52			
Gly3	5.79	9.3	2.87						
	(−10.9)								
[Ga^{III}(OEP)(Z-**cys**-Pro-Ala-Leu-OMe)] (**7**)[e]							10.32	4.20, 4.14	1.94
							(−44.6)	(41.2, 39.3)	(6.2)
Cys1	3.73	9.3	0.71	−0.77,					
	(−1.9)			−3.45					
Pro2	−		3.66	1.65	1.69,	2.42,			
					0.93	0.17			
Ala3	5.19	8.5	3.59	−0.48					
	(−51.1)								
Leu4	5.51	8.5	3.76	0.84,	0.25	0.25,			
	(−5.5)			0.45		−0.04			
[Ga^{III}(OEP)(Z-**cys**-Pro-Leu-OMe)] (**8**) [f]							10.31	4.22, 4.07	1.93
							(−46.0)	(39.2, 38.6)	(6.1)
Cys	3.65	8.5	0.62	−0.87,					
	(−1.4)			−3.24					
Pro2	−		3.78	1.75,	1.59,	2.30,			
				1.48	1.028	0.52			
Leu3	5.43	7.7	3.30	0.60,	0.36	0.19,			
	(−38.3)			0.05		0.11			

[a] ^{2}H NMR chemical shifts of the corresponding Fe(III) complexes in CH_2Cl_2 at 30 °C (15 mM) in parentheses. [b] ^{1}H NMR chemical shifts of the corresponding Fe(III) complexes in CD_2Cl_2 at 30 °C (15 mM) in parentheses. [c] Z-C_6H_5 (7.37−7.26), Z-CH_2 (4.92), OMe (3.45). The concentration is 20 mM. [d] Z-C_6H_5 (7.40−7.27), Z-CH_2 (4.91), OMe (3.48). The concentration is 20 mM. [e] Z-C_6H_5 (7.44−7.33), Z-CH_2 (5.09, 4.88), OMe (3.26). The concentration is 15 mM. [f] Z-C_6H_5 (7.46−7.38), Z-CH_2 (5.13, 4.92), OMe (3.21). The concentration is 15 mM.

Table 3. Temperature Coefficients of NMR Peaks Assignable to NH Protons ($-\Delta\delta/\Delta T$, ppb/K)[a] in $CDCl_3$[b]

comlexes	N(1)H	N(2)H	N(3)H	N(4)H
[Ga^{III}(OEP)(Z-**cys**-Leu-Gly-Leu-OMe)](**6**)[c]	0.1	∼0	−1.3	∼0
Z-Cys-Leu-Gly-Leu-OMe[d]	10.6	18.3	12.9	13.3
[Ga^{III}(OEP)(Z-**cys**-Leu-Gly-OMe)](**7**)[c]	2.9	0.5	1.3	−
Z-Cys-Leu-Gly-OMe	3.2	7.0	7.5	−
[Ga^{III}(OEP)(Z-**cys**-Pro-Ala-Leu-OMe)](**8**)[e]	1.3	−	1.0	1.6
Z-Cys-Pro-Ala-Leu-OMe[d]	2.9	−	6.6	1.6
[Ga^{III}(OEP)(Z-**cys**-Pro-Leu-OMe)](**9**)[e]	1.7	−	−1.5	−
Z-Cys-Pro-Leu-OMe[d]	3.4	−	1.6	−

[a] 303−228 K, every 15 K. [b] Data were obtained on a JEOL GSX-400 spectrometer as described in the Experimantal Section. [c] 15 mM. [d] 10 mM. [e] 20 mM.

mobility of each of the eight ethyl groups is not restricted because their peaks are not separated in the NMR time scale. Furthermore, calculation of rMM (restricted molecular mechanics) and rMD (restricted molecular dynamics) for **5**, **7** and **8** is carried out using the extensible systematic force field (ESFF) force field[65] but only with the rotational nuclear Overhauser effect (ROE) constraints. The average interproton distances from the analysis of the vacuum simulations of these complexes are in good agreement with their corresponding ROE-derived distances. Each of the Ga(III) complex structures is explained separately below.

[Ga^{III}(OEP)(Z-cys-Leu1-Gly-Leu2-OMe)] (5). The final set of ROE restraints for **5** consists of 22 constraints. The calculated structure of **5** possesses a small root-mean-square violation (RMSviol) (= 0.16 Å) (Figure 6a). Complex **5** has important ROE cross-peaks concerned with a turn conformation. The interresidue ROE cross-peaks are Leu1 C$^{\alpha}$H-Gly NH (medium), Leu1 C$^{\alpha}$H-Leu2 NH (medium), Gly NH-Leu2 NH (medium), Gly C$^{\alpha}$H1-Leu2 NH (medium), and Gly C$^{\alpha}$H2-Leu2 NH (medium). The average dihedral angles of the peptide backbone show that the family has β I-like turn conformation (Table 4).[53] rMM and rMD calculations of **5** show that the distance of S···H(N Leu1), S···H(N Gly), and S···H(N Leu2) are 2.57, 2.67, and 3.98 Å, respectively (Figure 6a). The short distances suggest the formation of the NH···S hydrogen bonds. The rMM and rMD results also correspond with the low-temperature coefficients of the amide protons (Table 3). The Ga−S−C−C dihedral angle is 158.9° by the steric hindrance between the porphyrin ring and the side chains of the leucine residues (Figure 6a). The backbone RMSD between 5 and the P-450cam

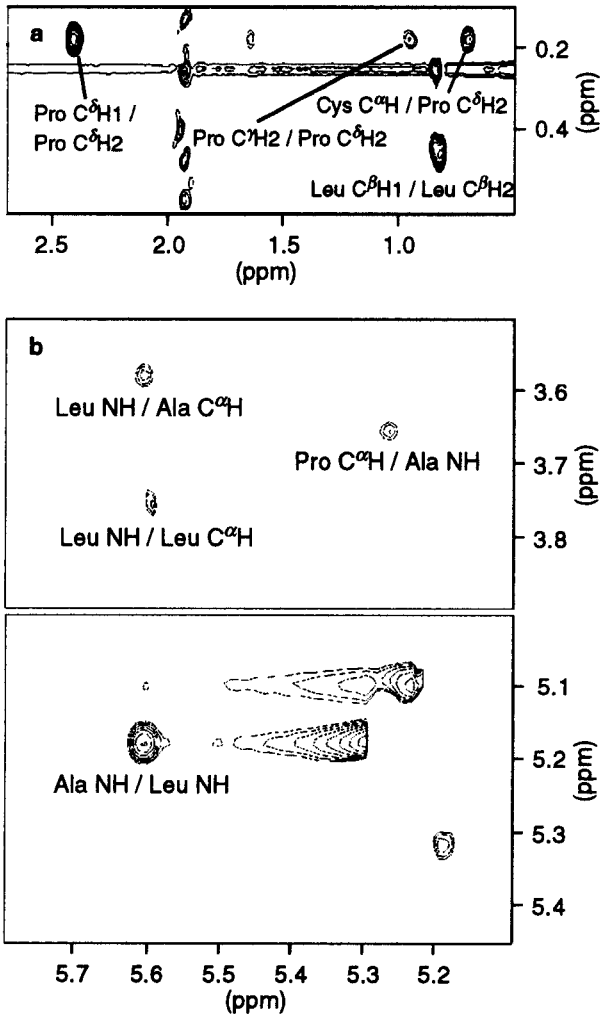

Figure 5. Partial 600-MHz ROESY spectrum of [Ga^{III}(OEP)(Z-**cys**-Pro-Ala-Leu-OMe)] (**7**) in $CDCl_3$ at 27 °C (20 mM). A 200-ms mixing time was used. The Pro C^{δ} and C^{γ} protons region (a) and the Ala and Leu NH region (b) are indicated.

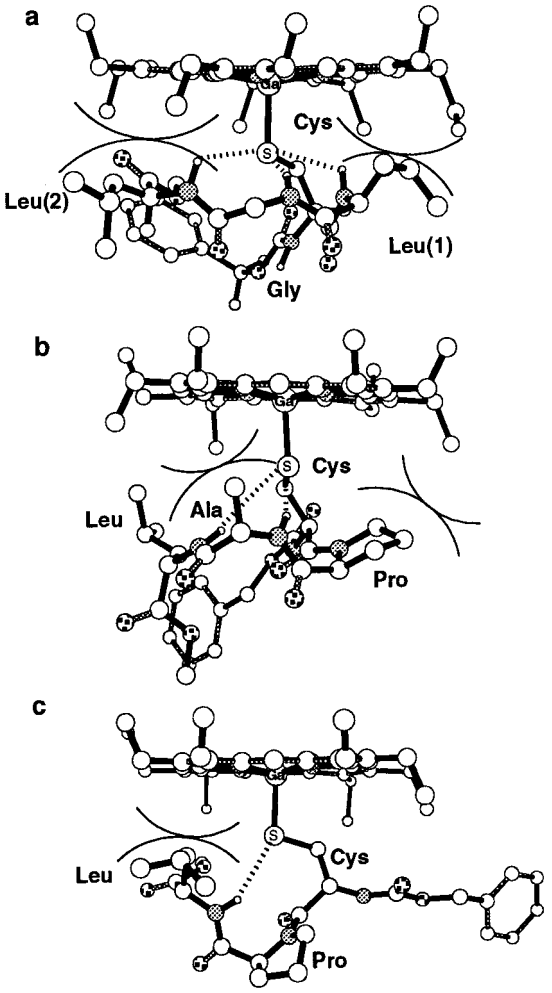

Figure 6. rMM and rMD structures of (a) [Ga^{III}(OEP)(Z-**cys**-Leu-Gly-Leu-OMe)] (**5**), (b) [Ga^{III}(OEP)(Z-**cys**-Pro-Ala-Leu-OMe)] (**7**), and (c) [Ga^{III}(OEP)(Z-**cys**-Pro-Leu-OMe)] (**8**).

Table 4. Averaged Dihedral Angles (deg) of the Conformation Families having the Lowest RMSviol among the Generated 50 Structures

residue	dihedral	**5**	**7**	**8**	P-450cam[a]	CPO[b]	β Type I[c]
Cys + 1	ϕ	−61.8	−53.0	−58.1	−73.6	−59.8	−60
	φ	−49.6	−33.4	−38.1	−24.8	−36.3	−30
Cys + 2	ϕ	−124.4	−84.6	−68.4	−83.0	−68.5	−90
	φ	−102.5	−55.8	−	12.6	−49.4	0

cysteine-ligand region is large (1.62 Å) (Figure 7a). The large RMSD indicates that the Cys-Leu-Gly-Leu fragment a very flexible.

[Ga^{III}(OEP)(Z-cys-Leu-Gly-OMe)] (6). The spectra of complex **6** have only limited ROE information about interresidue constraints because Leu $C^{\alpha}H$ and NH exhibit the same chemical shifts (Table 2). Therefore, we could not determine the solution structure of the peptide part by the rotational nuclear Overhauser effect spectroscopy (ROESY) experiment. We are thus proposing the solution structures based on the other experimental data, e.g., IR and ^2H NMR.

[Ga^{III}(OEP)(Z-cys-Pro-Ala-Leu-OMe)] (7). For the rMM and rMD calculations of **7**, 33 ROE restraints were used. The final structure of **7** satisfies the experimental restraints (RMSviol = 0.16 Å) (Figure 6b). A strong ROE between Cys $C^{\alpha}H$ and Pro C^{δ} protons (Figure 5a) shows that the Cys-Pro peptide bond has kept a *trans*-conformation.[66] The average dihedral angles and the ROE correlations of Ala NH-Leu NH (strong), Pro $C^{\alpha}H$−Ala NH (medium), and Ala $C^{\alpha}H$-Leu NH support the type I β turn-like conformation.[53,67] The calculated structure of **7** has short distances between cysteinyl sulfur atom and the amide protons of Ala NH (2.58 Å) and Leu NH (3.28 Å) (Figure 6b). The formation of NH···S hydrogen bonds is also supported by the ROEs, Cys$C^{\beta}H1$−Ala HN and Cys$C^{\beta}H1$-Leu HN, and the small temperature coefficients (Table 3). The peptide backbone indicates the small deviation from the CPO backbone (0.33 Å) (Figure 7b). Thus, the Cys-Pro-Ala-Leu fragment of **7** has a more rigid turn than the Cys-Leu-Gly-Leu of **5**. The Ga−S−C−C dihedral angle (146.3°) was determined by the steric hindrance among the porphyrin and the side chains of alanine and leucine residues (Figure 6b).

[Ga^{III}(OEP)(Z-cys-Pro-Leu-OMe)] (8). The structure of **8**, which was calculated by 34 ROE constraints, is shown in Figure 6c. The structure also has small RMSviol (0.17 Å). Complex **8**

(64) It is estimated that the OEP ring has less steric hindrance between the peptide and the porphyrin side chain than a tetraphenylporphyrin ring based on the preliminary Discover calculations for the Ga(III) peptide complexes.

(65) *Insight II User Guide, October 1995*; Biosym/MSI: San Diego, 1995.

(66) Wüthrich, K.; Braun, M. B. W. *J. Mol. Biol.* **1984**, *180*, 715−740.

(67) Wagner, G.; Neuhaus, D.; Worgotter, E.; Vasak, M.; Kägi, J. H. R.; Wüthrich, K. *J. Mol. Biol.* **1986**, *187*, 131−135.

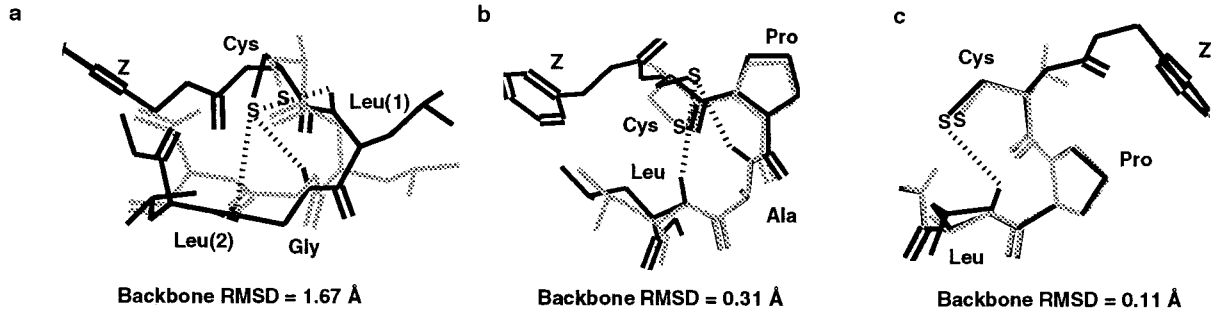

Figure 7. The superimposition of the Ga(III) complexes on the native proteins for (a) **5** and P-450cam;[25] (b) **7** and CPO[3]; and (c) **8** and CPO. The peptide backbones of Ga(III) complexes are shown as black lines, and the native proteins are shown as gray lines.

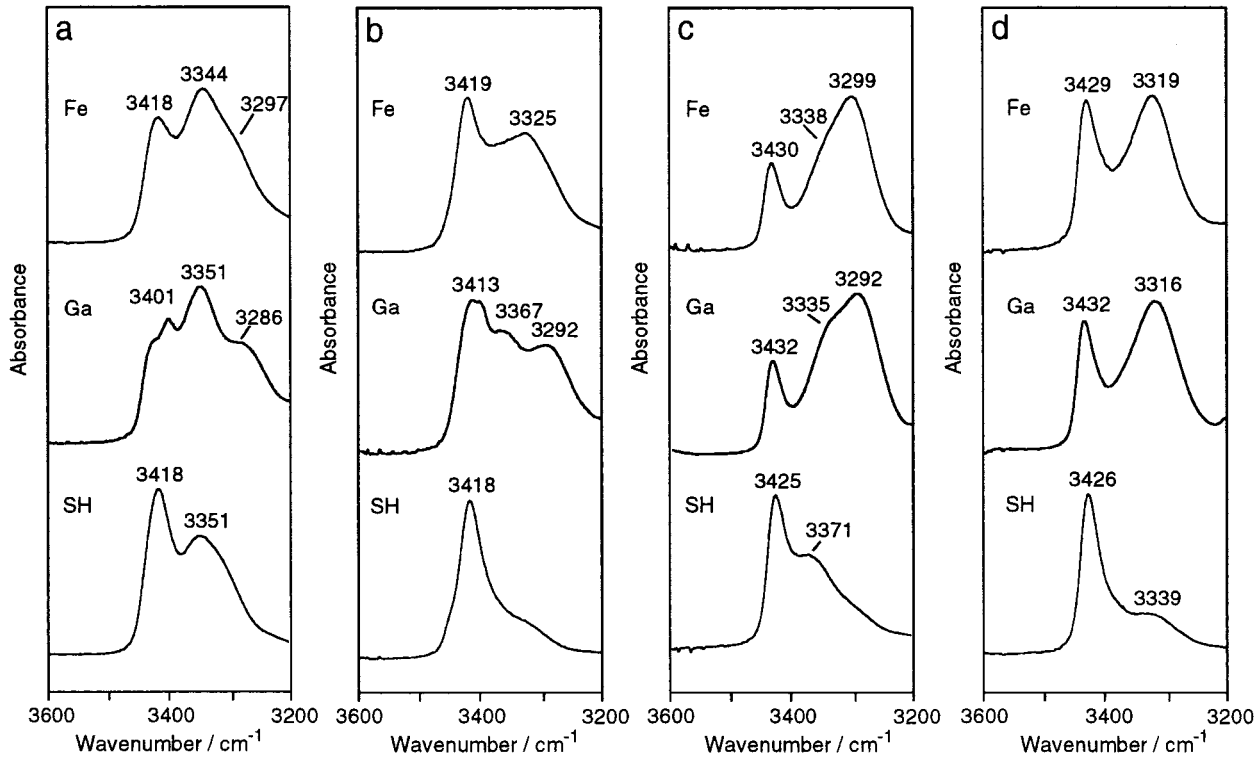

Figure 8. IR spectra of amide NH stretching region of (a) [Fe^{III}(OEP)(Z-**cys**-Leu-Gly-Leu-OMe)] (**1**) (top), [Ga^{III}(OEP)(Z-**cys**-Leu-Gly-Leu-OMe)] (**5**) (middle), Z-Cys-Leu-Gly-Leu-OMe (bottom), (b) [Fe^{III}(OEP)(Z-**cys**-Leu-Gly-OMe)] (**2**) (top), [Ga^{III}(OEP)(Z-**cys**-Leu-Gly-OMe)] (**6**) (middle), Z-Cys-Leu-Gly-OMe (bottom), (c) [Fe^{III}(OEP)(Z-**cys**-Pro-Ala-Leu-OMe)] (**3**) (top), [Ga^{III}(OEP)(Z-**cys**-Pro-Ala-Leu-OMe)] (**7**) (middle), Z-**cys**-Pro-Ala-Leu-OMe (bottom), and (d) [Fe^{III}(OEP)(Z-**cys**-Pro-Leu-OMe)] (**4**) (top), [Ga^{III}(OEP)(Z-**cys**-Pro-Leu-OMe)] (**8**) (middle), Z-Cys-Pro-Leu-OMe (bottom) in $CDCl_3$ (10 mM) through 1.0-mm path length at 26 °C.

was confirmed to have a *trans* conformation as deduced from the ROE cross-peak between CysC^{α}H and ProC^{δ}H1[66] and the ^{13}C NMR chemical shifts of ProC^{δ} and C^{γ}. The average dihedral angles of **8** show the type I β turn like conformation[53] such as **7** (Table 4). The temperature coefficient of Leu NH (−1.5 ppb/K) (Table 3) and S···HN(Leu) distance (3.00 Å) of the calculated structure (Figure 6c) indicate the formation of an intramolecular NH···S hydrogen bond. The small RMSD (0.11 Å) from the observed CPO conformation indicates that the proline residue plays an important role to keep the NH···S hydrogen bond in **8**.

IR Spectra. Figure 8 shows the NH stretching region of the IR spectra for the Fe(III), the Ga(III) complexes, and the corresponding peptides in $CDCl_3$ solution. A concentration of 10 mM was used here because 10−20 mM solutions were used for ^1H and ^2H NMR experiments. The intense band at ∼3420 cm^{-1} in $CDCl_3$ corresponds to non−hydrogen-bonded ν(NH) whereas the broader band at ∼3380 cm^{-1} reflects the presence of hydrogen-bonded species. The similarity of spectra between the Fe(III) complexes and the corresponding Ga(III) complexes indicates that the Fe(III) complexes have a hydrogen-bonding pattern similar to the corresponding Ga(III) complexes.

In the less polar solvent, e.g., $CDCl_3$, Ga(III) complexes, **5**−**8**, indicate several hydrogen-bonded peaks that are formed intramolecularly because the ^1H NMR temperature dependence of amide protons is less than 3.0 ppb/K (Table 3). In addition, the solution structures of the Ga(III) complexes show that the cysteinyl sulfur atom is adjacent to the backbone amide NH. The previous IR works for the NH···S hydrogen bond in alkanethiolate complexes indicated that the hydrogen-bonded ν(NH) is observed by the absorption at 3350 Å|3300 cm^{-1}.[33,37] Thus, the lowered ν(NH) values for **1**−**8** in the hydrogen bonding region are caused by the intramolecular NH···S hydrogen bonding but not by intermolecular NH···O═C bonding. Although the corresponding free peptides also have ν(NH)s in the hydrogen bond region, their NH temperature coefficients (Table 3) suggest that the hydrogen bonds are formed intermolecularly between NH and C═O. These results show the different hydrogen bond pattern between these cysteinyl thiolate complexes and the corresponding thiols.

Furthermore, the IR spectra of Fe(III) and Ga(III) complexes indicate interesting sequence dependence. The hydrogen-bonded ν(NH)s at 3351 and 3286 cm^{-1} of [Ga^{III}(OEP)(Z-**cys**-Leu-Gly-Leu-OMe)] (**5**) are little different from those of [Ga^{III}(OEP)(Z-**cys**-Leu-Gly-OMe)] (**6**) (3367 and 3292 cm^{-1}) (Figure 8a and b). The hydrogen-bonded ν(NH) of [Ga^{III}(OEP)(Z-**cys**-Pro-Ala-Leu-OMe)] (**7**) (3292 cm^{-1}) is 24 cm^{-1} lower than that of [Ga^{III}(OEP)(Z-**cys**-Pro-Leu-OMe)] (**8**) (3316 cm^{-1}). Information obtained by intensity of the free ν(NH) relative to the hydrogen-bonded ν(NH) is consistent with the conclusion from the room-temperature equilibrium constants of $K = [NH_{bonded}]/[NH_{free}]$, which were determined by us for these complexes.[68] Thus, the largest observed intensity of **3** shows formation the strongest intramolecular hydrogen bond.[69] These IR data suggest that the Cys-Pro-Ala-Leu fragment makes stronger intramolecular NH···S hydrogen bonds than the Cys-Leu-Gly-Leu fragment in their Fe(III) and Ga(III) complexes.

^{2}H NMR Spectra. ^{2}H NMR experiments were performed to confirm the presence of NH···S hydrogen bonds for the model Fe(III) complexes. Although the existence of the NH···S hydrogen bond has been suggested for heme-thiolate and iron−sulfur proteins,[3,70] it is very difficult to detect the hydrogen-bonded NH peaks by ^{1}H NMR spectroscopy because of the relaxation by the paramagnetic iron in native proteins.[38,56] Summers et al.[71] observed the NH···S hydrogen bond with use of ^{1}H-^{113}Cd heteronuclear multiple quantum coherence (HMQC) spectroscopy for ^{113}Cd-substituted rubredoxin. On the other hand, the chemical shifts of the hydrogen-bonded amides were determined (+40 to −40 ppm) for some paramagnetic model complexes,[31,72] by ^{2}H NMR.[73] Thus, we used ^{2}H NMR to detect these amide protons of **1**−**4** and [Fe^{III}(OEP)(Z-**cys**-Leu-OMe)] (Figures 9 and 10). The ^{2}H signals of their backbone amides were observed at an extreme upfield (ca. −50 to −10 ppm) by the formation of NH···S hydrogen bonds.

The values of amide N^{2}H chemical shifts of **1**−**4** do not agree with the observed trend of amide NH chemical shifts of the corresponding gallium complexes (Table 2). La Mar et al.[74] reported that the isotropic shifts of high-spin 5-coordinated complexes are mainly dominated by the contact shift. The net ring current effect estimated by the NH chemical shifts of the diamagnetic gallium complexes amounts to only a few part per million (listed in Table 2). Thus, large upfield shifts of the N^{2}Hs of the model Fe(III) complexes are caused by the contact shift through the NH···S hydrogen bond, and the chemical shifts reflect strength of the NH···S hydrogen bond in the Fe(III) complexes as already for some of the rubredoxin peptide model Fe(II) complexes.[35,72]

[Fe^{III}(OEP)(Z-**cys**-Leu-Gly-Leu-OMe)] (**1**) and [Fe^{III}(OEP)(Z-**cys**-Leu-Gly-OMe)] (**2**) shows four and three N^{2}H peaks, respectively (Figure 9a and b). The lowest shifted peak at 0.7 ppm among them is assigned to the Leu(2) N^{2}H of **1**. The difference between **2** and [Fe^{III}(OEP)(Z-**cys**-Leu-OMe)] suggests that the Gly and the Leu N^{2}Hs of 2 is observed at −10.9 and −18.8 ppm, respectively (Figure 9b). Therefore, the N^{2}Hs of cys, Leu(1), Gly, and Leu(2) can be observed at −5.7, −18.7, −9.8, and 0.7 ppm, respectively. The N^{2}H chemical shifts correspond to the S···HN distances of the rMM structure of [Ga^{III}(OEP)(Z-**cys**-Leu-Gly-Leu-OMe)] (**5**). For [Fe^{III}(OEP)(Z-**cys**-Pro-Ala-Leu-OMe)] (**3**) and [Fe^{III}(OEP)(Z-**cys**-Pro-Leu-OMe)] (**4**), three and two peaks are observed, respectively (Figure 10). The comparison between **3** and **4** indicates that the NH peaks of the residues, cys, Ala, and Leu, of **3** are observed at −1.9, −5.5, and −51.1 ppm, respectively. The chemical shift of Leu N^{2}H of **4** indicated 12.8 ppm lower shift from **3**. The observed lowfield shift suggests the weakening of NH···S hydrogen bond.[13,31,72] The result agrees with the information from the IR data and the proposed peptide solution structures of **7** and **8**. Therefore, the fourth residue contributes cooperatively to the regulation of the strength of NH (third residue)···S hydrogen bond.

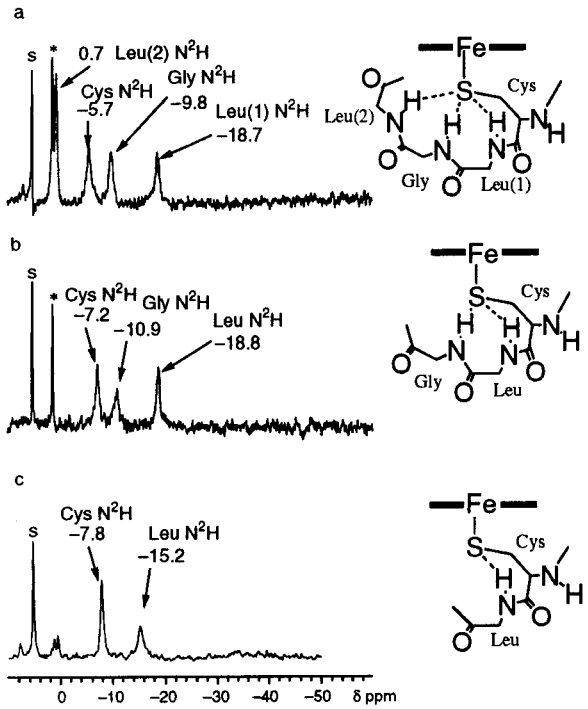

Figure 9. The 77-MHz ^{2}H NMR spectra of (a) [Fe^{III}(OEP)(Z-**cys**-Leu-Gly-Leu-OMe)] (**1**), (b) [Fe^{III}(OEP)(Z-**cys**-Leu-Gly-OMe)] (**2**), and (c) [Fe^{III}(OEP)(Z-**cys**-Leu-OMe)] in CH_2Cl_2 at 30 °C. An asterisk and 's' are peaks of impurity and solvent, respectively.

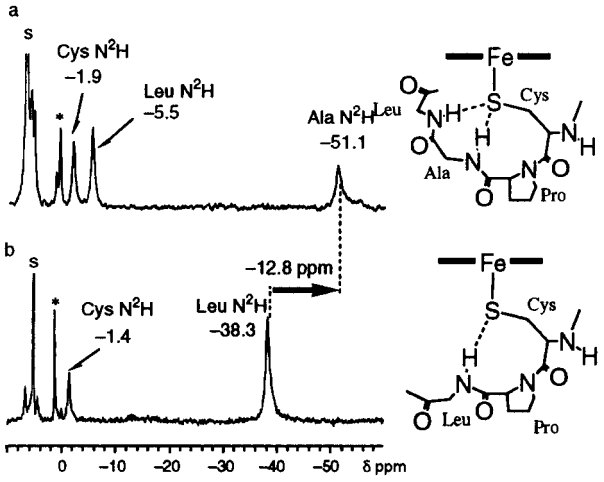

Figure 10. The 77-MHz ^{2}H NMR spectra of (a) [Fe^{III}(OEP)(Z-**cys**-Pro-Ala-Leu-OMe)] (**3**) and (b) [Fe^{III}(OEP)(Z-**cys**-Pro-Leu-OMe)] (**4**) in CH_2Cl_2 at 30 °C. An asterisk and 's' are peaks of impurity and solvent, respectively.

(68) **1**−**8** have the *K* values of 2.47, 1.48, 4.60, 2.02, 2.61, 1.61, 5.19, and 2.68, respectively.

(69) Hadzi, D.; Bratos, S. *The Hydrogen Bond*; Schuster, P., Zundel, G.; Sandorfy, C., Ed.; North-Holland Publishing Company: Amsterdam, 1976; Vol. II, pp 565−611.
(70) Adman, E.; Watenpaugh, K. D.; Jensen, L. H. *Proc. Natl. Acad. Sci. U.S.A.* **1975**, *72*, 4854−4858.
(71) Blake, P. R.; Lee, B.; Summers, M. F.; Park, J.-B.; Zhou, Z. H.; Adams, M. W. W. *New. J. Chem.* **1994**, *18*, 387−395.
(72) Ueyama, N.; Sun, W. Y.; Nakamura, A. *Inorg. Chem.* **1992**, *31*, 4053−4057.

Table 5. Redox Potentials of Fe^{III}/Fe^{II} for [Fe^{III}(OEP)(cys-peptide)] in Dichloromethane

complexes	$E_{1/2}$[a]	ΔE_p[b]	i_{pc}/i_{pa}
[Fe^{III}(OEP)(Z-**cys**-Leu-Gly-Leu-OMe)] (**1**)	−0.585	0.11	0.85
[Fe^{III}(OEP)(Z-**cys**-Leu-Gly-OMe)] (**2**)	−0.612	0.12	0.73
[Fe^{III}(OEP)(Z-**cys**-Pro-Ala-Leu-OMe)] (**3**)	−0.647	0.14	0.79
[Fe^{III}(OEP)(Z-**cys**-Pro-Leu-OMe)] (**4**)	−0.683	0.08	0.90
P-450_{cam} in H_2O[c]	−0.415		

[a] V vs SCE. [b] $\Delta E_p = E_{pa} - E_{pc}$. [c] The value reported by Fisher et al.[86] is converted to the value vs SCE.

Electrochemical Property. All the Fe(III) cys-containing peptide complexes described here exhibit quasireversible redox couples of [Fe^{III}(OEP)(cys-peptide)]/[Fe^{II}(OEP)(cys-peptide)] in dichloromethane at room temperature as listed in Table 5. The formation of specific NH···S hydrogen bonds has been proven to cause the positive shift of the redox potential of not only cys-containing peptide complexes[33,72] but also arenethiolate model complexes, [Fe^{III}(OEP)(S-2-$CF_3CONHC_6H_4$)].[13] Hence, the number and strength of NH···S hydrogen bonds have some influence on the redox potential of the Fe(III) complexes with porphinato and cys-containing peptides. The Fe^{III}/Fe^{II} redox potential of **1** [at −0.585 vs saturated calomel electrode (SCE)] is slightly more positive than that of **2** (−0.612 V). In **4**, the redox potential at −0.683 V was negatively shifted compared with that of **3** (−0.647 V). Thus, the tetrapeptide complexes have slightly more positive shifted redox potentials (30−40 mV) than the corresponding tripeptide complexes; this result is apparently correlated to the number of NH···S hydrogen bonds as detected by ^{2}H NMR.

Discussion

Fe(III) and Ga(III) Cys-containing Peptide Complexes as the Active Site Model of P-450 and CPO. Some examples of stable high-spin 5-coordinated Fe(III) cys-containing peptide complexes are now synthesized based on importance of invariant sequences in the proteins. The tetra- and tripeptide complexes containing some of the invariant sequences are kinetically more stable than the dipeptide model complexes that are converted to [Fe^{II}(OEP)] immediately in CH_2Cl_2 at 30 °C. The stability depends on the pK_a values of the cys-containing peptide, because the Fe(III) model complex is decomposed by the disulfide formation (eq 2). The solution structures of Ga(III) complexes (Figure 6) and ^{2}H NMR experiments of Fe(III) complexes (Figures 9 and 10) indicate the existence of the same intramolecular NH···S hydrogen bonds for **1**−**4**, but [Fe^{III}(OEP)-(Z-**cys**-Leu-OMe)] has only one NH···S hydrogen bond. In general, the hydrogen bond significantly contributes to the stabilization of the thiolate anion against the disulfide formation,[75] because the hydrogen bond can lower the pK_a values for the thiol and then reduces the potentiality for electron-transfer reduction of iron(III).[32] Actually, the tetra- and tripeptides having P-450 and CPO invariant fragments possess lower pK_a values than those of the dipeptides in micellar solution, for example, comparison among, Z-Cys-Leu-Gly-Leu-OMe (pK_a = 9.9), Z-Cys-Leu-Gly-OMe (9.0), and Z-Cys-Leu-OMe (11.2).[50] In addition, the intramolecular hydrogen bond forms only in the thiolate anion state,[32,75] whereas the corresponding thiol peptide instead form intermolecular NH···O═C hydrogen bonds as detected by ^{1}H NMR (Table 3) and IR (Figure 8). On the other hand, Ogoshi et al.[24] reported that Fe(OEP)(SR) complexes with R = alkyl are much less stable than Fe(OEP)(SPh) in organic solvents. Various 'S^--tails'[9,10,76] and 'S^--bridged'[11,12,77] model complexes have also been reported to depress the dissociation of the iron−sulfur bond. The proposed stabilizing mechanism of the Fe(III) state for the arenethiolate[13,16,20,23] and the artificial chelated[10,11] complexes seems to be different from those of P-450 and CPO because the native proteins have no such chelate- or arene-thiolate ligands. Thus, the NH···S hydrogen bond in the invariant fragments, Cys-Leu-Gly-Gln and Cys-Pro-Ala-Leu, may be one of the factors to stabilize the coordination of the cysteinyl thiolate anion to Fe(III) ion in the active site of P-450 and CPO.

Ga(III) cys-containing peptide complexes were also synthesized by the analogous ligand exchange reaction from Ga(OEP)-(OMe). These complexes are stable in $CHCl_3$ because the Ga(III) complexes are redox-inactive. CD (Figure 4) and IR (Figure 8) spectra indicate that peptide conformation of the Ga(III) complexes is very similar to that of the corresponding Fe(III) compounds caused by the NH···S hydrogen bonds.

The Structural Feature of the Invariant Fragments, Cys-Leu-Gly-X and Cys-Pro-Ala-Leu. The Cys-X-Gly (X = hydrophobic amino acid) sequences are highly conserved among "Classical P-450s" and NO-synthases.[2] The sequence, Cys-Pro-Ala, of CPO has also been preserved in iron−sulfur proteins, e.g., Cys-Pro-X (X = hydrophobic amino acid).[29,46,47] Thus, the invariant sequences of P-450 and CPO play an important role in the regulation of the Fe−S bonding. The peptide conformational analysis (Table 4) indicates that the invariant fragments of the Ga(III) complexes keep the hairpin turn conformation (β type I like).

The ϕ, φ dihedral angles of the Cys-Leu1-Gly-Leu2 sequence are quite different from those of the native P-450cam (Table 4 and Figure 7) because of the flexibility at the third glycine residue. Actually, the fourth Leu residue can hardly contribute to the formation of NH···S hydrogen bonds (Figure 8) because of the inherent flexibility. The Ga−S−C−C dihedral angle (158.9°) obtained using the rMM and rMD structure (Figure 6) is larger than that of the native P-450cam (87.0°) because of the steric hindrance among side chains of Leu1 and Leu2 and the porphyrin ring. The interaction was observed as the upfield shift of the Leu Cδ protons (Table 2) and as the ROE cross-peaks (data not shown). From the crystal structures of P-450cam,[4] we find that each of the two carbonyl groups of Gly359 and Gln360 give rise to two NH···O═C hydrogen bonds with NHs of the backbone of the N terminus of the following α-helix. In addition, the Cys carbonyl makes a hydrogen bond with the side chain amide of Gln360 in the native P-450cam. Thus, a particular conformation at the Cys357-Leu358-Gly359-Gln360 of P-450 is probably induced by the side chain of Gln360 and by the following α-helix, although the model complex, [Ga-(OEP)(Z-**cys**-Leu-Gly-Leu-OMe)], is quite flexible in solution.

On the other hand, the ϕ, φ dihedral angles of the Cys-Pro-Ala-Leu sequence are similar to those of the native CPO (Table 4 and Figure 7). The tripeptide complex **8** has smaller RMSD than the tetrapeptide complex **7** because proline is strongly favored in the position $i + 1$ of a β turn, because of its reduced conformational freedom.[53] The peptide hairpin turn conformation having the NH···S hydrogen bond is analogous to the familiar

(73) Hebendanz, N.; Kohler, F. H.; Scherbaum, F.; Schlesinger, B. *Magn. Reson. Chem.* **1989**, *27*, 798−802.
(74) LaMar, G. N.; Eaton, G. R.; Holm, R. H.; Walker, F. A. *J. Am. Chem. Soc.* **1973**, *95*, 63−75.
(75) Okamura, T.; Takamizawa, S.; Ueyama, N.; Nakamura, A. *Inorg. Chem.* **1998**, *37*, 18−28.
(76) Collman, J. P.; Groh, S. E. *J. Am. Chem. Soc.* **1982**, *104*, 1391−1403.
(77) Battersby, A. R.; Howson, W.; Hamilton, A. D. *J. Chem. Soc., Chem. Commun.* **1982**, 1266−1268.

β-turn (Type I−III), which contains the intramolecular NH···O═C hydrogen bond.[70] The interaction between the Pro or Ala side chains and the porphyrin ring was detected by the remarkable upfield shift of the ProCδ and Ala Cβ protons (Table 2). The results suggest that the hairpin turn conformation at the Cys-Pro-Ala-Leu fragments, which has two NH···S hydrogen bonds, is kept by the rigid proline residue in the active site of CPO.

The flexibility of the invariant sequences, Cys-Leu-Gly-X and Cys-Pro-Ala-Leu, contributes to the catalytic reactions of P-450. The proposed catalytic cycle[6] of P-450cam involves various steps in which the cysteinyl thiolate basicity must be changed by the binding of a substrate, O_2 or putidaredoxin, to promote the catalysis.[78−81] The flexible invariant sequence is considered to be suitable to control the basicity of cysteinyl thiolate at each of the steps. In contrast, the halogenation of CPO involves the high-spin 5-coordinated Fe(III) state and only two intermediates in the cycle.[6] Therefore, CPO prefers the rigid fragment, Cys-Pro-Ala-Leu, to stabilize just three states, i.e., (Por)Fe^{III}, ($Por^{+\bullet}$)-Fe^{IV}═O, and (Por)Fe^{III}−OCl.

The Relationship between the Invariant Sequence to the Reactivity of P-450 and CPO. We focus here only on the effect of invariant sequence for the Fe^{III}/Fe^{II} redox potential of P-450 to initiate the monooxygenation. Several other factors that can contribute to the regulation of the redox potential are (1) the polarity of the heme environment,[82−85] (2) spin-state equilibrium which is switched by the aqua ligand at the heme coordination site,[25,86] and (3) the delicate difference in electronic structure of the heme macrocycle.[87,88]

The tetrapeptide complexes, **1** and **3**, indicate the slightly positive shift by 30−40 mV from the redox potentials of the tripeptide complexes, **2** and **4**, respectively. The observed difference between the tetra- and the tripeptide complexes is caused by the number and strength of NH···S hydrogen bonds which are confirmed by ^{2}H and IR spectroscopies. Such a positive shift of redox potential due to the NH···S hydrogen bond has already been reported for various alkanethiolates,[36,37] cys-containing peptide complexes,[33,35,72,89] and iron−sulfur proteins.[70,90,91] For complex **1**, the additional NH···S hydrogen bond of Leu2 contributes to the 27-mV positive shift from **2**. For CPO models, the stronger NH(Ala)···S of **3** makes a 36-mV positive shift from **4**. The values are smaller than those of the reported hydrogen-bonded models.[31,33,35−37,72,89] Thus, the invariant fragments of P-450 and CPO give a little contribution to the regulation of the high-spin Fe^{III}/Fe^{II} redox potential by the formation of NH···S hydrogen bonds.

It is well-known that CPO structures bears no similarity to P-450 at either the primary or the tertiary structural level.[3] Nevertheless, the Cys ligand in CPO is situated at the N-terminus of an α-helix and forms the NH···S hydrogen bond, just as in P-450.[45] Thus, the α-helical dipole interaction probably plays an important role for the regulation of the catalytic activities through the NH···S hydrogen bond.[92] Further investigation of this point is underway.

Conclusion

Fe(III) cys-containing peptide heme complexes have been synthesized as P-450 and CPO models to examine the role of the NH···S hydrogen bond; their redox behaviors were obtained from the three-dimensional solution structure by ROESY experiments and by restrained molecular dynamics calculations using the NMR constraints of the corresponding Ga(III) complexes. Our results indicate that each of the invariant fragments of P-450, Cys-Leu-Gly, and of CPO, Cys-Pro-Ala-Leu, forms the intramolecular NH···S hydrogen bonds, and the strength of such hydrogen bonds is caused by the preferred hairpin turn conformation of these cys-containing peptide fragments. The peptide conformation contributes to kinetic stabilization of the high-spin Fe(III)(cys-peptide) resting state rather than the positive shift of the Fe^{III}/Fe^{II} redox potential.

Experimental Section

Materials. All operations were performed under an argon atmosphere. Dichloromethane, methanol-d^1, and all other solvents were purified by distillation before use. Fe^{III}(OEP)(OMe) and Ga^{III}(OEP)(OMe) were prepared according to the methods in the literature.[42,49] Peptide ligand synthesis is described in Supporting Information.

[Fe^{III}(OEP)(Z-cys-Leu-Gly-Leu-OMe)] (1). [Fe^{III}(OEP)(OMe)] (5.6 mg, 9.0×10^{-3} mmol) and Z-Cys-Leu-Gly-Leu-OMe (5.1 mg, 9.0×10^{-3} mmol) were dissolved in CH_2Cl_2 with stirring. After the solution was evaporated to dryness, black powder was obtained. MS (ESI) Calcd (found) *m*/*e*: {[Fe(OEP)(Z-**cys**-Leu-Gly-Leu-OMe)] + H^+}, 1140.6 (1140.1).

[Fe^{III}(OEP)(Z-cys-Leu-Gly-OMe)] (2). 2 was obtained from [Fe^{III}-(OEP)(OMe)] (5.6 mg, 9.0×10^{-3} mmol) and Z-Cys-Leu-Gly-OMe (4.0 mg, 9.0×10^{-3} mmol) as for complex **1**. MS (ESI) Calcd (found) *m*/*e*: {[Fe(OEP)(Z-cys-Leu-Gly-OMe)] + H^+}, 1027.5 (1027.5).

[Fe^{III}(OEP)(Z-cys-Pro-Ala-Leu-OMe)] (3). 3 was also obtained by the reaction of [Fe^{III}(OEP)(OMe)] (5.6 mg, 9.0×10^{-3} mmol) with Z-Cys-Pro-Ala-Leu-OMe (5.0 mg, 9.0×10^{-3} mmol) as for complex **1**. MS (ESI) Calcd (found) *m*/*e*: {[Fe(OEP)(Z-**cys**-Pro-Ala-Leu-OMe)]+H^+}, 1138.5 (1138.6).

[Fe^{III}(OEP)(Z-cys-Pro-Leu-OMe)] (4). 4 was prepared from [Fe^{III}-(OEP)(OMe)] (5.6 mg, 9×10^{-3} mmol) and Z-Cys-Pro-Leu-OMe (4.3 mg, 9×10^{-3} mmol) as for complex **1**. MS (ESI) Calcd (found) *m*/*e*: {[Fe(OEP)(Z-**cys**-Pro-Leu-OMe)]+H^+}, 1166.9 (1166.9).

[Ga^{III}(OEP)(Z-cys-Leu-Gly-Leu-OMe)] (5). 5 was prepared by a modification of the reported ligand-exchange reaction.[42] A dichloromethane solution (2 mL) of [Ga^{III}(OEP)(OMe)] (13.9 mg, 0.022 mmol) was added to a dichloromethane solution (2 mL) of Z-Cys-(SH)-Leu-Gly-Leu-OMe (12.2 mg, 0.022 mmol). The mixture was stirred for 30 min and then concentrated under reduced pressure. UV−vis (dichloromethane): 351 nm (40 000 M^{-1} cm^{-1}), 413 nm (235 000), 538 nm (17 500), and 575 nm (18 600). MS (ESI) Calcd (found) *m*/*e*: {[Ga(OEP)(Z-**cys**-Leu-Gly-Leu-OMe)]+H+}, 1153.5 (1153.2).

(78) Gaul, E. M.; Kassner, R. J. *Inorg. Chem.* **1986**, *25*, 3734−3740.
(79) Chottard, G.; Schappacher, M.; Ricard, L.; Weiss, R. *Inorg. Chem.* **1984**, *23*, 4557−4561.
(80) Shiro, Y.; Iizuka, T.; Makino, R.; Ishimura, Y.; Morishima, I. *J. Am. Chem. Soc.* **1989**, *111*, 7707−7711.
(81) Unno, M.; Christian, J. F.; Benson, D. E.; Gerber, N. C.; Sligar, S. G.; Champion, P. M. *J. Am. Chem. Soc.* **1997**, *119*, 6614−6620.
(82) Rodgers, K. K.; Sligar, S. G. *J. Am. Chem. Soc.* **1991**, *113*, 9419−9421.
(83) Kessner, R. J. *J. Am. Chem.Soc.* **1973**, *95*, 2674−2677.
(84) Gunner, M. R.; Alexov, E.; Torres, E.; Lipovaca, S. *JBIC* **1997**, *2*, 126−134.
(85) Mauk, A. G.; Moore, G. R. *J. Biol. Inorg. Chem.* **1997**, *2*, 119−125.
(86) Fisher, M. T.; Sligar, S. G. *J. Am. Chem. Soc.* **1985**, *107*, 5018−5019.
(87) Reid, L. S.; Lim, A. R.; Mauk, A. G. *J. Am. Chem. Soc.* **1986**, *108*, 8197−8201.
(88) Koga, H.; Sagara, Y.; Yaoi, T.; Tsujimura, M.; Nakamura, K.; Sekimizu, K.; Makino, R.; Shimada, H.; Ishimura, Y.; Yura, K.; Go, M.; Ikeguchi, M.; Horiuchi, T. *FEBS Lett.* **1993**, *331*, 109−113.
(89) Ohno, R.; Ueyama, N.; Nakamura, A. *Inorg. Chem.* **1991**, *30*, 4887−4891.
(90) Adman, E. T. *Biochim. Biophys. Acta* **1979**, *549*, 107−144.
(91) Charles, W.; Carter, J. *X-ray Analysis of HiPIP and Ferredoxin*; Academic Press: New York, 1977; Vol. III.
(92) This manuscript was submitted just after the paper (Ueno, T.; Kousumi, Y.; Nakajima, K.; Yoshizawa-Kumagaye, K.; Ueyama, N.; Okamura, T.; Nakamura, A. *J. Am. Chem. Soc.* **1998**, *120*, 12264−12273) was accepted.
(93) Hasemann, C. A.; Ravichandran, K. G.; Peterson, J. A.; Deisenhofer, J. *J. Mol. Biol.* **1994**, *236*, 1169−1185.

[Ga^{III}(OEP)(SR)] {**RS = Z-cys-Leu-Gly-OMe (6), Z-cys-Pro-Ala-Leu-OMe (7) and Z-cys-Pro-Leu-OMe (8)**}. **6**−**8** were synthesized by the method mentioned above. **[Ga^{III}(OEP)(Z-cys-Leu-Gly-OMe)]** (**6**). UV−vis (dichloromethane) 350 nm (38 000), 411 nm (236 000), 538 nm (16 500), and 575 nm (17 100). MS (ESI) Calcd (found) *m*/*e*: {[Ga(OEP)(Z-**cys**-Leu-Gly OMe)] + H^+}, 1040.5 (1040.1). **[Ga^{III}-(OEP)(Z-cys-Pro-Ala-Leu-OMe)] (7).** UV−vis (dichloromethane) 351 nm (41 000), 411 nm (250 000), 539 nm (17 000), 576 nm (18 000). MS (ESI) Calcd (found) *m*/*e*: {[Ga(OEP)(Z-**cys**-Pro-Ala-Leu-OMe)] + H^+}, 1151.5 (1150.9). **[Ga^{III}(OEP)(Z-cys-Pro-Leu-OMe)] (8).** UV−vis (dichloromethane) 350 nm (40 000), 413 nm (234 000), 538 nm (13 700), and 575 nm (18 100). MS (ESI) Calcd (found) *m*/*e*: {[Ga-(OEP)(Z-**cys**-Pro-Leu-OMe)]+H^+}, 1080.5 (1080.0).

Preparation of N^{2}H-Substituted Fe(III) Porphyrin Complexes. The amide N^{2}H-substituted peptide ligands were obtained by the deuteration of the SH-deprotected (SH-free) peptides with methanol-d_1.[72] N_2H-substituted Fe(III) porphyrin complexes were synthesized by the reaction of [Fe^{III}(OEP))(OMe)] with the corresponding amide N^{2}H-substituted SH-free peptide ligand by the same method described above for the synthesis of complex **1**.

Physical Measurements. UV−visible spectra were recorded on a Shimadzu UV3100PC. CD and MCD measurements were recorded on a Jasco J-720w spectropolarimeter equipped with an electromagnet operated at 1.5 T. These measurements were carried out using a 0.1- and 0.01-cm cell path at ca. 30 °C. The measurements of cyclic voltammograms in dichloromethane solution were carried out on a BAS 100 B/W instrument with a three-electrode system: a glassy carbon working electrode, a Pt-wire auxiliary electrode, and a SCE. The scan rate was 100 mV/s. The concentration of the sample was 2 mM, containing 200 mM of *n*-Bu_4NClO_4 as a supporting electrolyte. Potentials were determined at room temperature vs a SCE as a reference. Mass spectrometric analyses were performed on a Finniganmat LCQ-MS instrument in acetonitrile/dichloromethane. IR spectra were taken on a JASCO IR-8300 spectrometer with a NaCl cell with a 1.0-mm path length. NMR spectroscopy and related computational procedures are described in Supporting Information.

Acknowledgment. We are grateful for financial support by JSPS Fellowships [for T.U.; grant 2691(1995−1998)] and by a Grant-in Aid for Specially Promoted Research from the Ministry of Education, Science and Culture (for A.N.; grant 06101004). We also thank Dr. R. Kataoka (Ryoka Systems Inc.) for NMR solution structural calculations. We acknowledge Professor S. Kaizaki, Department of Chemistry, Graduate School of Science, Osaka University, for CD and MCD spectral measurements.

Supporting Information Available: Preparation of the cysteine-containing peptides, details of NMR spectroscopy, and computational procedures, electronic and MCD spectral data (Tables S1 and S2), ^{1}H NMR spectra for **3**, **7**, and the corresponding peptide (Figure S1), superimposed rMM and rMD structures for **5**, **7**, and **8** (Figure S2), and cyclic voltammograms of **1** and **3** (Figure S3). This material is available free of charge via the Internet at http://pubs.acs.org.

IC980710U